

See discussions, stats, and author profiles for this publication at: <https://www.researchgate.net/publication/231654016>

Self-Assembly and Tribological Property of a Novel 3-Layer Organic Film on Silicon Wafer with Polydopamine Coating as the Interlayer

ARTICLE in THE JOURNAL OF PHYSICAL CHEMISTRY C · NOVEMBER 2009

Impact Factor: 4.77 · DOI: 10.1021/jp9073416

CITATIONS

39

READS

24

5 AUTHORS, INCLUDING:



Junfei Ou

Nanchang Hangkong University of Aeronautics

60 PUBLICATIONS 876 CITATIONS

[SEE PROFILE](#)



Jinqing Wang

Chinese Academy of Sciences

103 PUBLICATIONS 1,805 CITATIONS

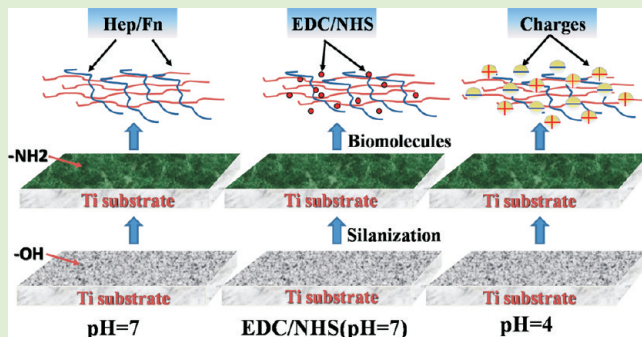
[SEE PROFILE](#)

Tailoring of the Titanium Surface by Immobilization of Heparin/Fibronectin Complexes for Improving Blood Compatibility and Endothelialization: An in Vitro Study

Guicai Li, Ping Yang,* Yuzhen Liao, and Nan Huang

Institute of Biomaterials and Surface Engineering, Key Laboratory for Advanced Technologies of Materials, Ministry of Education, Southwest Jiaotong University, Chengdu 610031, P.R. China

ABSTRACT: To improve the blood compatibility and endothelialization simultaneously and to ensure the long-term effectiveness of the cardiovascular implants, we developed a surface modification method, enabling the coimmobilization of biomolecules to metal surfaces. In the present study, a heparin and fibronectin mixture (Hep/Fn) covalently immobilized on a titanium (Ti) substrate for biocompatibility was investigated. Different systems [*N*-(3-dimethylaminopropyl)-*N'*-ethylcarbodiimide and *N*-hydroxysuccinimide, electrostatic] were used for the formation of Hep/Fn layers. Atomic force microscopy (AFM) showed that the roughness of the silanized Ti surface decreased after the immobilization of Hep/Fn. Fourier transform infrared spectroscopy (FTIR), Toluidine Blue O (TBO) test, and immunochemistry assay showed that Hep/Fn mixture was successfully immobilized on Ti surface. Blood compatibility tests (hemolysis rate, APTT, platelet adhesion, fibrinogen conformational change) showed that the coimmobilized films of Hep/Fn mixture reduced blood hemolysis rate, prolonged blood coagulation time, reduced platelets activation and aggregation, and induced less fibrinogen conformational change compared with a bare Ti surface. Endothelial cell (EC) seeding showed more EC with better morphology on pH 4 samples than on pH 7 and EDC/NHS samples, which showed rounded and aggregated cells. Systematic evaluation showed that the pH 4 samples also had much better blood compatibility. All results suggest that the coimmobilized films of Hep/Fn can confer excellent antithrombotic properties and with good endothelialization. We envisage that this method will provide a potential and effective solution for the surface modification of cardiovascular implant materials.



INTRODUCTION

A truly biocompatible biomaterial should perform its function without causing undue host response or resulting adverse clinical reaction.¹ As regards cardiovascular implants that contact blood directly, such as pacemaker components, heart valves, and endovascular stents,² blood compatibility is the first consideration, especially in the early stages after implantation. As an initial reaction to an implanted biomaterials, the adsorption of plasma proteins and the adhesion of platelets may induce thrombus formation and implant failure. Endothelialization is another consideration, particularly for long-term implantation. Implants completely covered by endothelial cells (ECs) will not cause thrombotic events and will perform their function for extended periods. Late thrombosis with adverse clinical outcomes occurs when stent endothelialisation is delayed or absent.³

Many efforts to enhance the biocompatibility of cardiovascular biomaterials have been explored, including heat treatment,⁴ coating device materials with biocompatible films (such as DLC,⁵ Ti-O,⁶ and polymers^{7,8}), and immobilizing biomolecules (heparin,⁹ chitosan¹⁰). In addition, direct endothelial cell seeding and endothelialization¹¹ using biomolecules (tropoelastin,¹² collagen,¹³

and RGD peptides¹⁴) is also considered a useful method for improving biocompatibility, although the limited stability of biomolecules *in vivo* is still a drawback to clinical translation. Even though blood compatibility and endothelialization of implants have been greatly improved, the previous studies have shown that anticoagulation and endothelialization simultaneously are contradictory processes. In general, when blood compatibility is improved with anticoagulation molecules, the growth of EC will be inhibited,¹⁵ whereas when the growth of EC is promoted with extracellular matrix molecules, blood compatibility declines.^{16,17} Therefore, most current studies focus only on one aspect of biocompatibility: blood compatibility or endothelialization, and few studies have investigated both aspects simultaneously.^{18,19} However, the development of biomaterials that can inhibit thrombus formation and accelerate endothelialization simultaneously will inevitably have major significance for the long-term implantation of biomedical devices.

Received: December 5, 2010

Revised: January 24, 2011

Published: February 18, 2011

In this study, Ti plates were chosen as the substrates because Ti and its alloy are widely used for cardiovascular implants.²⁰ We report on the surface modification of Ti using alkali activation (NaOH) and silanization with γ -aminopropyltriethoxysilane (APTE) for obtaining amino reactive groups, which can be used to immobilize covalently biomolecules.²¹ There are many different methods for the immobilization of biomolecules onto a surface, for example, physical adsorption, encapsulation, entrapment, and covalent binding. The advantages of covalent immobilization are that immobilized biomolecules are not easily removed by physical force (e.g., rinsing) and are robust enough to withstand in vivo exposure, although the bioactivity of the biomolecules may be influenced. To the best of our knowledge, biomaterials covalently modified with different biomolecules can retain the properties of the biomolecule used.²² The immobilization of different biomolecules on biomaterial surfaces has been proven to improve blood compatibility¹⁰ or to enhance cell attachment and proliferation.²³ Usually, the method for immobilizing biomolecules consists of two steps: one biomolecule is first immobilized, and then the second biomolecule is attached,²² but the bioactivity of the first immobilized biomolecule may be influenced by the succeeding biomolecule immobilization process. The simultaneous coimmobilization of different biomolecules could avoid this problem, especially because each biomolecule has a chance to be exposed to target proteins or cells, although this is rarely reported.²⁴ Therefore, the coimmobilization of anticoagulant and endothelialized biomolecules is postulated to improve blood compatibility and accelerate endothelialization of biomaterials simultaneously. Here two biomolecules, heparin and fibronectin, were chosen as the components for simultaneous coimmobilization. Heparin is an important anticoagulant clinically for minimizing thrombus formation on artificial surfaces²⁵ and is capable of interacting with numerous proteins associated with cell attachment (e.g., fibronectin, vitronectin) and with proliferation.²⁶ Heparin has an incontrovertible effect on inhibiting thrombus formation by catalytically increasing the binding rate of antithrombin III (ATIII) to thrombin.²⁷ Covalent immobilization of heparin and chitosan on PLA was shown to reduce platelet adhesion and increase fibroblasts attachment.¹⁰ The effect of heparin immobilization on endothelial cell proliferation is not consistent^{15,28} with inhibition or promotion. Fibronectin (440 kD) is an extracellular matrix protein known to promote cell attachment, spreading,²⁹ differentiation,³⁰ and phagocytosis³¹ through its arginine-glycine-asparagine (RGD) sequence. Fibronectin immobilized on silanized Ti surface was found to enhance the attachment of fibroblasts.²¹ Fibronectin can also participate in platelet adhesion and aggregation via specific integrin receptors on the platelet membrane.³² However, heparin and fibronectin can form complexes (Hep/Fn) under physiological conditions by heparin binding to a site on the fibronectin chain; this binding could combine individual biological functions. The simultaneous coimmobilization of heparin and fibronectin is thus anticipated to promote both anticoagulant effect and endothelialization. Two systems for the formation of Hep/Fn were chosen: one was the *N*-(3-dimethylaminopropyl)-*N'*-ethylcarbodiimide and *N*-hydroxysuccinimide (EDC/NHS) cross-linking system. EDC/NHS can activate carboxyl acid groups and promote their covalent binding to amino groups; this has been proved to be noncytotoxic³³ and biocompatible.³⁴ The immobilization of heparin to EDC/NHS cross-linked collagen was proved to improve in vivo blood compatibility by Wissink et al.,³⁵ but the influence of EDC/NHS on endothelialization was

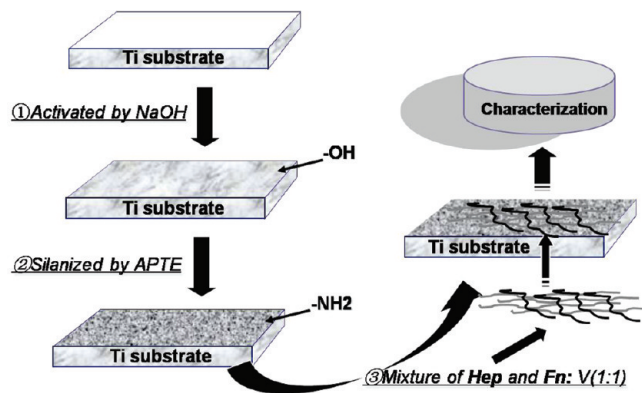


Figure 1. Sketch map of the preparation of Hep/Fn coimmobilization films on Ti substrate.

not clear, although new, untried cross-linkers may also cause problems. A complex of heparin and fibronectin is thus formed by binding of the activated carboxyl groups on heparin to the amino groups on fibronectin. Another approach is to use electrostatic attraction, typically used for layer-by-layer assembly (LbL). The deposition of heparin/chitosan by the LbL method was shown to improve the biocompatibility of a coronary stent system¹⁹ and also antibacterial properties.³⁶ However, most biomolecules used in LbL are polysaccharides or polyelectrolytes, whereas few reports refer to ECM proteins, which would have useful important roles in cell attachment and proliferation. Relevant to our study is that heparin carries a net negative charges even at very low pH, whereas the isoelectric point of fibronectin is ~ 5.5 , and thus heparin and fibronectin form complexes through electrostatic attraction at appropriate pH values. After the formation of Hep/Fn, complexes were immobilized on silanized Ti surfaces. The aim of this work was to develop a ready to use surface on metallic or other inorganic substrates, possessing both anticoagulation and endothelialization properties.

In the present work, we demonstrate the construction and evaluation of coimmobilized Hep/Fn films on Ti substrate for surface modification for blood-contacting devices. The modification of the Ti substrate was characterized by AFM, FTIR, and contact angle measurement, and the quantity of immobilized heparin and fibronectin deposited was investigated by TBO and immunochemistry, respectively, to determine if the coimmobilization of the Hep/Fn mixture improved biocompatibility, hemolysis rate, contact activation, and the deposition of blood platelets; endothelial cells seeding and proliferation was also studied. The effects of these coimmobilized Hep/Fn films on the simultaneous improvement of the blood compatibility and endothelialization are first investigated here *in vitro*, however, it is anticipated that this Hep/Fn coatings will have potential for improving the biocompatibility of clinical blood-contacting biomaterial devices.

MATERIALS AND METHODS

Materials and Reagents. Ti substrates (10×10 mm) were prepared using 99.5% pure Ti foils (Baoji, China). Ultrapure water (>18.2 M Ω , Millipore Milli-Q system) was used in the experiments. Phosphate buffer saline (PBS, 0.067 M, pH 7.3) was purchased from Hyclone and adjusted to pH 4 with HCl. H_2SO_4 (1 M) in PBS was used as a stop solution for immunochemistry assay. *N*-Hydroxy-2,5-dioxo-pyridine-3-sulfonicacid sodium salt (NHS, 1mM, purity: >99%), 5 mM

Table 1. Explanation of the Samples

sample ID	preparation of the samples
Ti	pristine titanium
TiOH	pristine Ti activated by NaOH
TiOHA	TiOH silanized by APTE
TiOAHF	TiOHA immobilized with Hep/Fn mixture
pH 7 (TiOAHF/pH 7)	TiOHA immobilized with Hep/Fn that mixed under physiological conditions
EDC/NHS (TiOAHF/EDC/NHS)	TiOHA immobilized with Hep/Fn that mixed under EDC/NHS cross-linking conditions
pH 4 (TiOAHF/pH 4)	TiOHA immobilized with Hep/Fn that mixed under electrostatic attraction conditions

1-ethyl-3-dimethylaminopropyl carbodiimide (EDC), γ -aminopropyltriethoxysilane (APTE), TBO, and acid orange 7 (AO) were purchased from Sigma-Aldrich. Heparin from porcine intestinal mucosa and fibronectin from human were purchased from Sigma-Aldrich. Mouse monoclonal antihuman Fn RGD antibody, mouse polyclonal antihuman Fn antibody, mouse monoclonal antihuman fibrinogen (FGN) γ chain antibody, horseradish peroxidase (HRP)-conjugated goat antimouse IgG antibody and TMB (3,3',5,5'-tetramethylbenzidine) for the ELISA tests were purchased from BD Biosciences, San Jose, CA. Fluorescein isothiocyanate (FITC)-labeled mouse polyclonal antihuman Fn antibody for Fn staining and Alcian blue 8GX for Hep staining were purchased from Sigma-Aldrich. An activated partial thromboplastin time (APTT) kit for the anticoagulation properties test was purchased from Sunbio, China. M199 culture medium and Alamar Blue reagent for EC culture and proliferation test were purchased from BD Biosciences, San Jose, CA. The actin staining reagent kit (SABC-FITC) for the EC cytoskeleton was purchased from Boshide, China. All other reagents used in the experiments were of the highest analytical purity (>99.9%).

Fabrication of Hep/Fn Coimmobilization films on Ti Substrate. Figure 1 shows the fabrication process of Hep/Fn coimmobilization films on Ti substrate. Ti foils were polished and ultrasonically cleaned twice in acetone, ethanol, and deionized water (dH_2O) for 5 min each and then were dried in an oven at 60 °C for 2 h before use. The cleaned Ti plates were immersed in 2.5 M NaOH solution at 80 °C for 24 h and then thoroughly rinsed with dH_2O and blown dry. This process produced a very hydrophilic substrate, which was then silanized by immersing into a 2% v/v solution of the APTE in 99.8% anhydrous ethanol for 10 h to generate an amino surface, and this surface was sonicated in ethanol for 5 min to remove the physisorbed molecules and to obtain the silane monolayer. The silanized surfaces were then functionalized by grafting the Hep/Fn mixture at 37 °C for 2 h and then rinsed with PBS to remove the unattached Hep and Fn molecules. Here 5 mg/mL Hep and 100 μ g/mL Fn in PBS were premixed with the volume ratio of 1:1 under different conditions before immobilization, that is, pH 7 (control), pH 4, and with EDC/NHS cross-linking, respectively. At pH 7, Hep can bind to the Hep binding site on Fn chains by hydrophobic interaction or hydrogen bond formation. At pH 4, Hep can bind to Fn by electrostatic interactions because of the negative charge on Hep and the positive charge on Fn ($pI_{(Fn)} \approx 5.5$). For EDC/NHS cross-linking, EDC and NHS were diluted in PBS (pH 7.3) and used within half an hour. $V_{(EDC/NHS)}/V_{(Hep/Fn)}$ used was 1:10. Hep here could bind to Fn by the interaction between activated carboxyl and amino groups on the Fn. Samples with Hep/Fn mixtures on Ti are denoted pH 7, pH 4, and EDC/NHS in the study. Ti substrate activated by NaOH is denoted TiOH, the silanized TiOH surface by APTE was denoted TiOHA, and the TiOHA surface immobilized with Hep/Fn mixture was denoted TiOAHF. Pristine Ti was used as the reference (Table 1).

AFM. The surface topography and roughness of the treated samples (pristine Ti, TiOH, TiOHA, and TiOHA coimmobilized with Hep/Fn) were investigated using a Nanowizard II AFM (JPK Instruments, Berlin, Germany) in tapping mode. AFM test was performed at room temperature

in air at a scan rate of 0.5 Hz using Si cantilevers. Image analysis was performed using the CSPM Imager software.

FTIR. FTIR can be used to identify pure compounds and any functionalities present by the vibrational modes of specific chemical bonds in the sample. The infrared absorption spectra of the pristine Ti and TiOHA coimmobilized with Hep/Fn were obtained using a Fourier transform infrared (FTIR, NICOLET 5700) spectrometer in diffuse reflectance mode. For each spectrum obtained, a total of 64 scans were accumulated at 4 cm^{-1} resolution. Scanning was conducted in the range from 400 to 4000 cm^{-1} .

The Acid Orange 7 (AO) Test. To determine the amine concentration of the surfaces, TiOHA samples were immersed in 500 $\mu\text{mol/L}$ AO-HCl (pH 3) solution dissolved in water in a 500 μL well. After shaking for at least for 5 h at 37 °C, the samples were rinsed three times with the pH 3 HCl solution. Then, the samples were immersed into pH 12 NaOH solution in a 500 μL well and shaken for 15 min at room temperature to dissolve the adsorbed AO. Finally, 150 μL of desorbed AO supernatant was added to a 96-well plate, and the optical density (OD) was recorded with a microplate reader (μ Quant, Biotek instruments) at 485 nm. The AO concentration was parallel to the amine concentration on the samples.

Contact Angle Measurement. Static (sessile drop) water contact angles (CAs) were determined with a contact angle apparatus (JY-82, China). Samples were fixed to a glass slide, and a droplet of Milli-Q water was added to the surface. The CA of each drop on the surface was recorded using a horizontal microscope; the equilibration time of the droplet was 3 s before the measurement. The mean value of the CA was calculated from at least three individual measurements taken at different locations on the examined samples.

Toluidine Blue O Assay. The amount of immobilized heparin on samples was determined by a TBO assay, as described by Smith et al.³⁷ In brief, the samples immobilized with heparin were incubated in 5 mL of a freshly prepared solution of 0.04 wt % TBO in aqueous 0.01 M HC1/0.2 wt % NaCl. Then, the samples were gently shaken at 37 °C for 4 h and rinsed twice with demineralized water; during this process, the Hep/TBO complex was formed on the sample surface. Following this, 5 mL of a 4/1 (v/v) mixture of ethanol and aqueous 0.1 M NaOH was added, and the Hep/TBO complex dissolved and was released into the fluid phase. After complete dissolution of the complex, 200 μL of supernatant was added to a 96-well plate, and the OD value was obtained with a microplate reader at 530 nm. The OD value was used to calculate the amount of immobilized heparin from a calibration curve.

The heparin calibration curve was prepared as follows: To a heparin solution of known concentration, the same volume of a freshly prepared TBO solution was added. The mixture was shaken at 37 °C for 4 h, and Hep/TBO complex precipitated. Then, the mixture was centrifuged at 3500 rpm for 10 min. Subsequently, the precipitate was rinsed with aqueous 0.01 M HC1/0.2 wt % NaCl and dissolved in 5 mL of a 4/1 (v/v) mixture of ethanol and aqueous 0.1 M NaOH. The OD value was obtained with a microplate reader at 530 nm.

Alcian Blue 8GX Staining-Heparin Qualitative Characterization. Alcian Blue staining was used to view the immobilized heparin

on the samples surface. The method reported elsewhere by Wissink et al.³⁵ was modified for our study. In brief, the samples were blocked with 1 wt % BSA in PBS at 37 °C for 1 h and rinsed with PBS. Then, a solution of Alcian Blue 8GX (2% w/v) in 3% acetic acid solution was added, and the samples were stained at 37 °C for 30 min. After washing five times with dH₂O (totally 15 min), the samples were observed by optical microscopy (Leica, Germany).

Immunochemistry Assay for the Quantity of Fn, the Exposure of Fn-RGD Exposure and FGN γ Chain. The quantity of bound Fn, the exposure of Fn-RGD exposure, and FGN γ chain on sample surface were all determined by an indirect immunochemistry method. In brief, the samples were first blocked with 1 wt % BSA in PBS at 37 °C for 30 min. Subsequently, the mouse monoclonal antihuman antibody (anti-Fn, Fn-RGD or FGN γ chain, diluted 1:250 in PBS) was added and incubated at 37 °C for 1 h; then, the samples were thoroughly rinsed three times with PBS. Thereafter, HRP conjugated goat anti-mouse IgG antibody (diluted 1:100 in PBS) was added and incubated at 37 °C for another 1 h. The samples were washed three times again with PBS. Furthermore, the 100 μL TMB solution was added on the sample surfaces and reacted in dark for 10 min (blue color), and then 50 μL of 1 M H₂SO₄ was used to stop the peroxidase-catalyzed reaction (yellow color). Finally, 130 μL supernatant was transferred to a 96-well plate, and the absorbance at 450 nm was measured on a microplate reader. The concentration of fibronectin and the degree of exposure of Fn-RGD or FGN γ chain was obtained by comparison with the calibration curve. All experiments were done in quadruplicate.

Fibronectin Qualitative Characterization. For the qualitative characterization of bound Fn, FITC-labeled mouse polyclonal antihuman Fn antibody was used to stain the immobilized Fn on sample surfaces. The procedure used was introduced as follows: The samples were first fixed with 2.5% glutaraldehyde in PBS at room temperature for 30 min and then blocked with 1 wt % BSA in PBS at 37 °C for 30 min. Subsequently, the FITC-labeled mouse polyclonal antihuman Fn antibody (diluted 1:100 in PBS) was added and incubated at 37 °C for 1 h; then, the samples were thoroughly rinsed five times with PBS. Finally, samples were observed using a fluorescence microscope (Leica, Germany).

Hemolysis Rate Test. The samples were immersed in diluted blood solution containing 2% fresh anticoagulated (ACD) human blood and 98% physiological salt solution and incubated at 37 °C for 1 h. After centrifugation at 3000 rpm for 5 min, the absorbance of the solution was recorded as D_t . Under the same conditions, the solution containing 2% ACD blood and 98% physiological salt solution was used as a negative reference, and the solution containing 2% ACD blood and 98% distilled water was used as a positive reference. These absorbances were recorded as D_{nc} and D_{pc} , respectively. The hemolysis rate α of the samples was calculated using the following formula

$$\alpha = \frac{D_t - D_{nc}}{D_{pc} - D_{nc}} \times 100$$

APTT. The anticoagulation property of the coimmobilized samples was determined by means of an APTT assay. Fresh frozen human platelet poor plasma (PPP) was thawed at 37 °C. PPP (500 μL) was added to the samples and incubated at 37 °C for 15 min. Then, 100 μL of incubated PPP was transferred to a test tube and 100 μL APTT reagent was added, followed by incubation at 37 °C for 3 min. Subsequently, 100 μL of an aqueous 0.025 M CaCl₂ solution was added. The suspension was stirred by a magnetic stirrer, and coagulation time was determined at 37 °C using a coagulation instrument (Hospitex Diagnostics, Italy).

Platelet Adhesion Test. A platelet adhesion test was used to evaluate the adhesion behavior and activation of the platelets on the samples. Fresh human whole blood was taken from a healthy volunteer and anticoagulated with 0.109 M solution of sodium citrate at a dilution ratio of 9:1 (blood/sodium citrate solution). Then platelet-rich plasma (PRP) was obtained by centrifuging anticoagulated blood at 1500 rpm for 15 min

at room temperature. After that, the samples were immersed in 500 μL of PRP and incubated at 37 °C for 1 h. Subsequently, the samples were rinsed thoroughly three times with PBS and fixed with 2.5% glutaraldehyde for 2 h. Then, the samples were then observed using SEM. Also, optical microscopy was used to image nine randomly chosen fields to obtain a statistical assessment of the quantity of adhered platelets.

Microscopy of Platelets by SEM. The surface morphology of the adhered platelets was examined using an environmental SEM (FEI Philips XL 30, Amsterdam, The Netherlands). The vacuum pressure for observation was 1×10^{-5} . All samples were successively dehydrated at increasing alcohol concentrations (50, 75, 90, and 100%; $V_{alcohol}/V_{demineralized\ water}$), dealcoholized at increasing isoamyl acetate (50, 75, 90, and 100%; $V_{isoamyl\ acetate}/V_{alcohol}$), and dried using a CO₂ critical point drier (CPD030, Balzers) and coated with 10 nm of gold before taking images. Images at different magnifications were collected for each sample.

Conformational change of the Exposure γ Chain of Fibrinogen (FGN). Exposure of the γ chain on FGN could lead to binding on the GPIIb/IIIa receptor on the platelet membrane and further cause the platelets aggregation. The exposure of the FGN γ chain was detected by immunochemistry, as previously described.

EC Culture. ECs derived from human umbilical vein were isolated and cultured by the following method. A human umbilical cord was cannulated and washed thoroughly with PBS to remove the blood inside the lumen; then, 0.1% type II collagenase (Gibco BRL) in medium 199 was introduced and incubated at 37 °C for 10 min. The detached cells were washed in serum-free medium and collected in complete M199 containing 20% fetal calf serum (FCS, Gibco BRL), 50 μg/mL ECGF (Sigma), 100 μg/mL heparin, 20 mmol/L HEPES, 2 mmol/L L-glu, 100 U/mL penicillin, and 100 μg/mL streptomycin. The suspended cells were then seeded in a single-use culture flask and incubated at 37 °C in a humidified atmosphere containing 95% air and 5% CO₂. Replicated cultures were performed by being trypsinized with trypsin in PBS buffer when cells approached confluence. Cells were fed with fresh prepared growth medium every 48 h. The third generation of EC was used to evaluate the proliferation behavior on samples.

Ti, TiOH, and TiOHA samples were sterilized in a steam autoclave at 120 °C for 2 h prior to EC culture experiments, and Hep/Fn mixtures were filtered and added to the TiOHA samples prior to EC culture experiments. Subsequently, all sterilized samples were placed in a 24-well culture plate, and 1 mL of EC suspension was added. The concentration of EC used for seeding was 7×10^4 cells/mL.

Alamar Blue Assay. EC proliferation was investigated by Alamar Blue assay after 1, 3, and 5 days of incubation, respectively. The medium was removed, and the samples were washed twice with PBS. Subsequently, fresh medium (without phenol red) containing Alamar Blue reagent was added to each sample and incubated at 37 °C for 3 h under standard culture conditions. Afterward, 200 μL of the blue solutions was transferred to a 96-well plate. The absorbance was measured at 570 and 600 nm by a microplate reader. All proliferation experiments were performed in quadruplicate.

Morphology of EC. To study the extent of cell spreading and cytoskeleton formation of EC on samples, we performed immunofluorescence staining of actin using SABC-FITC kit. ECs were seeded on the samples with the concentration of 7×10^4 cells/mL and incubated at 37 °C for 3 and 5 days, respectively. Then, all samples were washed with PBS, fixed with 2.5% glutaraldehyde for 2 h at room temperature, blocked in 1% BSA for 30 min, permeabilized in 0.1% Triton X-100 solution for 15 min, and then washed twice with PBS. Subsequently, the samples were incubated with a rabbit mAb antihuman actin antibody (diluted 1:100 in PBS) at 37 °C for 1 h and rinsed three times with PBS. Thereafter, the samples were incubated with a biotinylated goat anti-rabbit IgG antibody (diluted 1:100 in PBS) at 37 °C for 1 h and rinsed three times with PBS. After that, the samples were incubated with SABC-FITC (diluted 1:100 in PBS) at 37 °C for 1 h and rinsed five times with

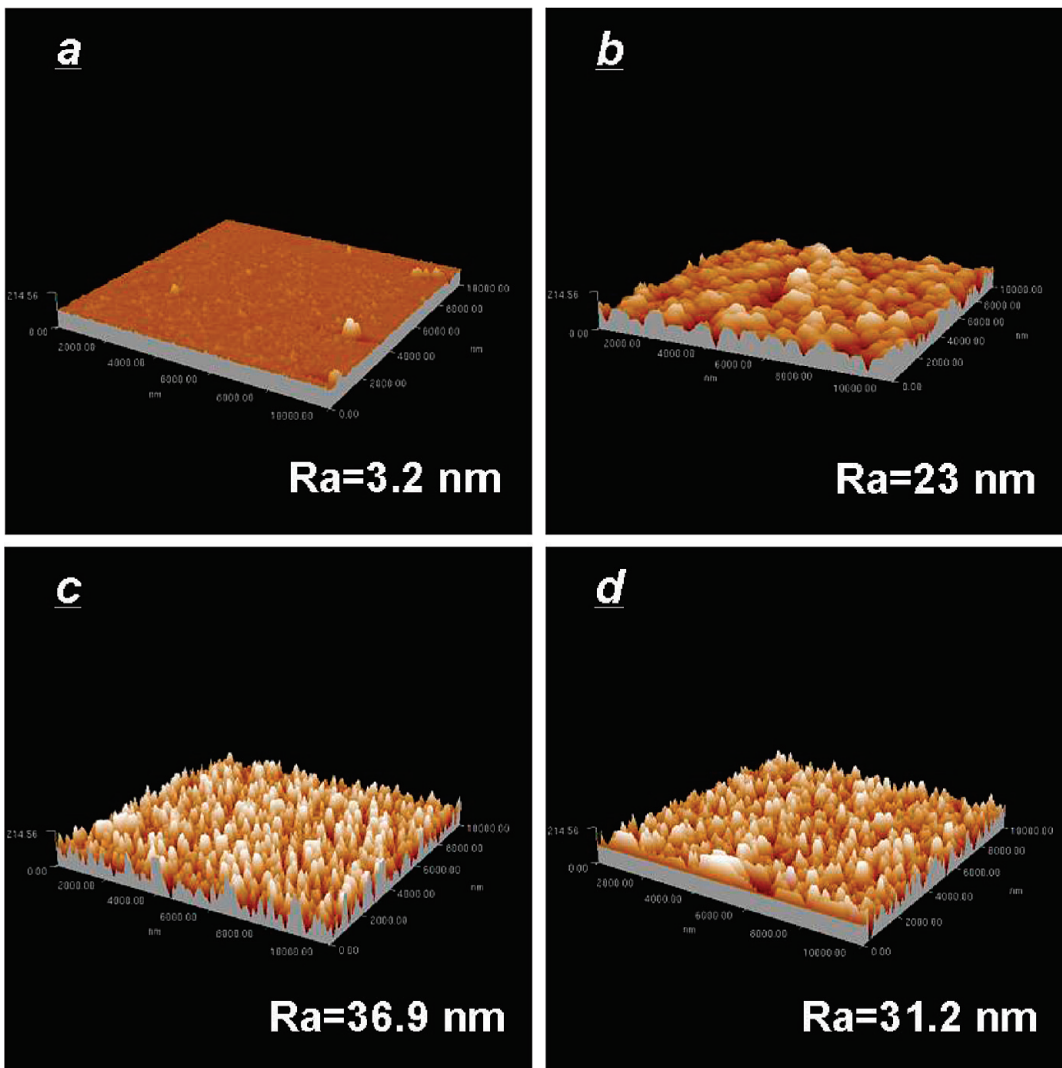


Figure 2. AFM of: (a) pristine Ti, (b) TiOH, (c) TiOHA, and (d) TiOAHF.

PBS. Finally, the samples were mounted in an aqueous medium with antifading agents and photographed using a fluorescence microscopy.

Conformational Change of Fn: Exposure of RGD Peptides. The conformational change of Fn, with exposure of RGD peptides (Fn III_{9–10}), could allow binding to the integrin receptor on the EC membrane and further promote their attachment. Such exposure of RGD peptides was detected by immunochemistry method, as previously described.

Data Analysis. The data were analyzed with software SPSS 11.5 (Chicago, IL). Statistical evaluation of the data was performed using a Student's paired *t* test. The probability (*P*) values *P*<0.05 were considered to be statistically significant. The results were expressed as mean \pm SD.

RESULTS

AFM and FTIR. Commonly, activation by NaOH causes roughening of the Ti surface, and the grafting of short chain alkyl, that is, APTE, further increases the surface roughness. The morphological change of the surface can be observed by AFM (Figure 2). Here different geometric features are demonstrated: the surface of the control Ti (Figure 2a) appears as almost uniformly flat with an average roughness (*R*_a) of 3.2 nm and becomes

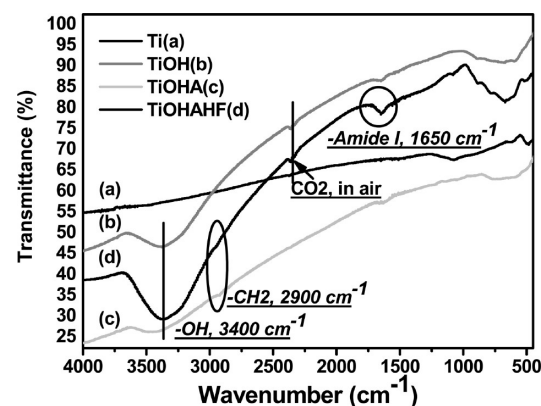


Figure 3. FTIR spectra of: (a) pristine Ti, (b) TiOH, (c) TiOHA, and (d) TiOAHF.

corrugated with short peaks and a roughness of 23 nm after etching by NaOH (Figure 2b). Then, a much rougher (36.9 nm) surface with higher peaks is obtained after grafting with APTE (Figure 2c), indicating the presence of APTE on the TiOH surface. The increased roughness might be caused by the cross-linking of APTE.

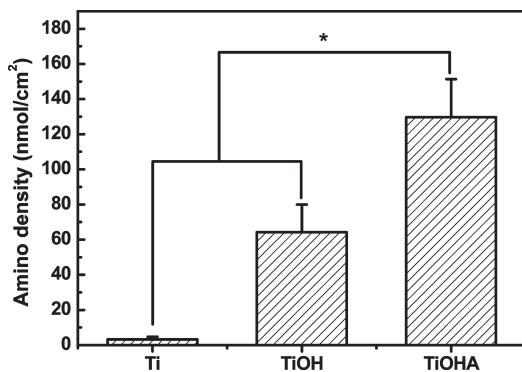


Figure 4. Surface amine concentration of pristine Ti, TiOH, and TiOHA (* $p < 0.05$ compared with TiOH and Ti, mean \pm SD, $N = 4$).

Table 2. Contact Angles of Water As a Function of Process of Ti Substrate^a

sample	contact angle (deg)
Ti	58.35 ± 0.95
TiOH	0.2 ± 0.03
TiOHA	28.45 ± 3.09
pH 7	6 ± 2.08^b
EDC/NHS	15.33 ± 2.08^b
pH 4	21 ± 2.26^b

^aWater contact angle indicated the TiOHAHF surface was hydrophilic.

^b $p < 0.05$ compared with TiOHA, mean \pm SD, $N = 4$.

However, the surface roughness of the Hep/Fn immobilized surface was reduced to 31.2 nm (Figure 2d), which could be due either to the filling of surface fits by heparin and fibronectin molecules or to the cross-linking caused by the binding of Hep/Fn mixture to APTE; however, this indicates the presence of heparin and fibronectin on the TiOHA surface. All of the NaOH activated, APTE grafted, and biomolecule-immobilized surfaces appeared to be uniform on larger scans of $10 \times 10 \mu\text{m}$ but nonhomogeneous at the submicrometer range. No morphological differences were observed between the samples of pH 7, pH 4 and EDC/NHS.

FTIR analysis, shown in Figure 3, indicates the presence of specific functional groups on the grafted surface. Compared with the original Ti surface (Figure 3a), the TiOH surface (Figure 3b) shows a new peak at 3400 cm^{-1} , which approximates to the $-\text{OH}$ group. The APTE grafted surface (Figure 3c) shows new peaks at 2900 cm^{-1} corresponding to $-\text{CH}_2$ and $-\text{CH}_3$, indicating an APTE derived surface. A reduced $-\text{OH}$ peak was observed compared with TiOH surface because of the reaction between the $-\text{OH}$ groups on substrate and those on APTE. However, the $-\text{NH}_2$ peak at 3200 cm^{-1} is not readily seen with FTIR and could not be found in the spectrum. The Hep/Fn-immobilized Ti surface (Figure 3d) shows a substantial amount of hydroxyl and amide groups, as indicated by the $-\text{OH}$ and $\text{C}=\text{O}$ stretching vibrations ($3400\text{--}3200$ and 1650 cm^{-1} , respectively). The peaks in 1650 cm^{-1} also appeared, and there was no any intensity change on TiOH and TiOHA, which could be ascribed to the residual water during the sample preparation, whereas the intensity of this peak increased on TiOHAHF. These findings indicate the presence of Hep/Fn on the Ti surface. However, it is difficult to distinguish the two biomolecules because of the overlapping carboxyl stretching vibrations ($1715\text{--}1650 \text{ cm}^{-1}$)

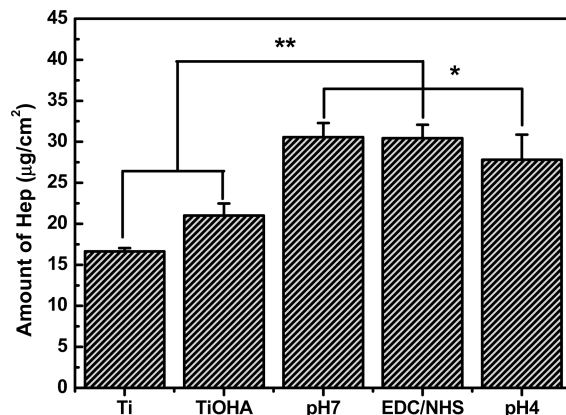


Figure 5. Quantitative characterization of heparin: determination of immobilized heparin on samples of pH 7, pH 4, and EDC/NHS by TBO test, pristine Ti, and TiOHA were used as reference (** $p < 0.05$ compared with Ti and TiOHA; * $p > 0.05$ among different Hep/Fn-immobilized samples; mean \pm SD, $N = 4$).

on heparin and the amide groups (1650 cm^{-1}) on the fibronectin. No significant difference was observed among the samples of pH 7, EDC/NHS, and pH 4, and only a representative FITR spectrum of TiOHAHF is shown.

Determination of Amine Concentration by the AO test. Quantitative results for amine concentrations on the surfaces were obtained using the AO test, shown in Figure 4. Compared with the Ti and TiOH surfaces, TiOHA showed a significantly higher ($p < 0.05$) amino concentration of $>65 \text{ nmol}/\text{cm}^2$. Note that there were also more amino groups of $>60 \text{ nmol}/\text{cm}^2$ on TiOH than on Ti, which could be ascribed to the physical adsorption of AO to the rough surface of TiOH.

Contact Angle. The contact angle for water was measured as a function of Ti substrate processing (Table 2). Compared with Ti, water contact angles dramatically decreased to $\sim 0^\circ$ after etching with NaOH, then increased to $26.5 \pm 3.6^\circ$ after silanization by APTE, indicating that the TiOHA surfaces were more hydrophobic than TiOH surfaces. The contact angles of all Hep/Fn coimmobilized samples increased in the order of: pH 7 $<$ EDC/NHS $<$ pH 4. In comparison, all of the Hep/Fn coimmobilized samples were more hydrophilic than the TiOHA surface.

Quantitative and Qualitative Characterization of Heparin. The amount of heparin immobilized was determined by the TBO method at room temperature. Figure 5 shows the amount of bonded heparin on the sample of pH 7, pH 4, and EDC/NHS. It is clear that the binding of heparin on the foregoing samples was significantly greater than that on the Ti and TiOHA surfaces ($p < 0.05$), whereas no significant difference was shown between the samples of pH 7, pH 4, and EDC/NHS, with at least 7 to $8 \mu\text{g}/\text{cm}^2$ of heparin immobilized on these samples.

Alcian Blue is a cationic dye and can be used for selective staining of glycosaminoglycans. Light microscopy images of Alcian-Blue-stained Hep/Fn films of pH 7, pH 4, and EDC/NHS (Figure 6) demonstrate homogeneous staining through the entire surface, in contrast with the unstained surface of TiOHA using the same procedure. The results also indicate that heparin was successfully immobilized on the samples. No obvious difference was observed on the samples, which corresponded well with the TBO results.

Quantitative and Qualitative Characterization of Fibronectin. Figure 7 shows the surface concentration of Fn on different samples determined by immunochemistry. Compared with the pristine Ti and TiOHA samples, a significantly higher ($p < 0.05$)

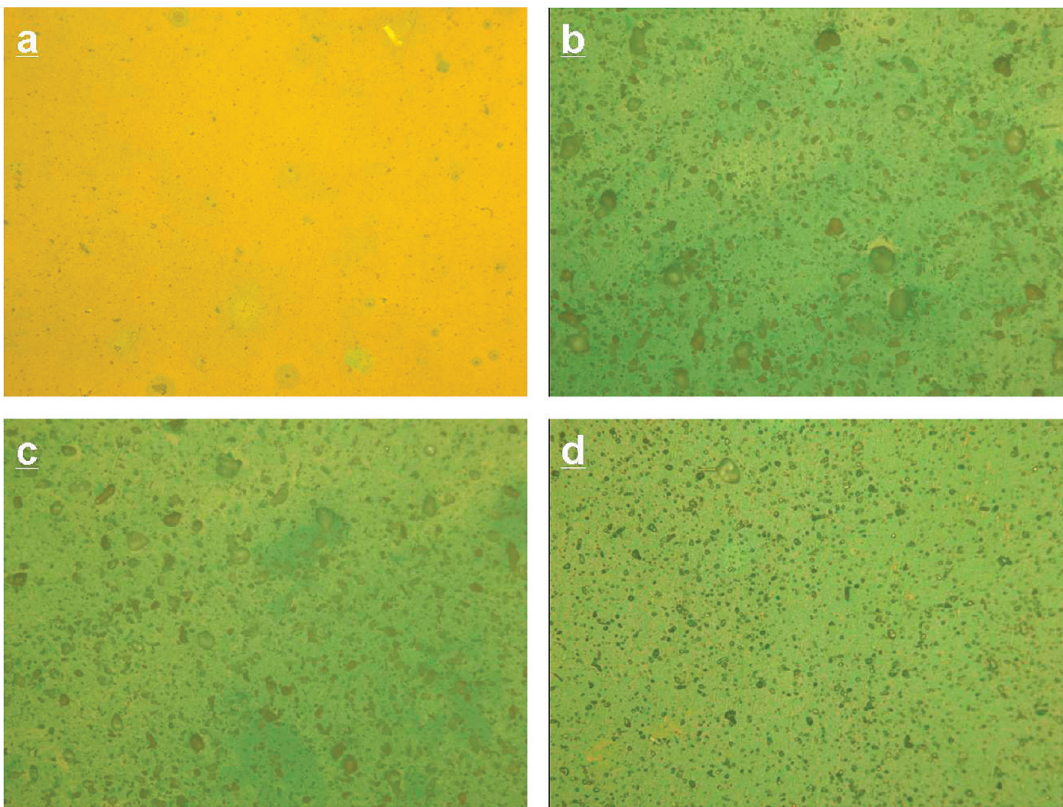


Figure 6. Qualitative characterization of heparin: light microscopic images of Alcian-Blue-stained heparin sections of immobilized Hep/Fn on Ti surface: (a) TiOHA, (b) pH 7, (c) EDC/NHS, and (d) pH 4 (original magnification: 20 \times).

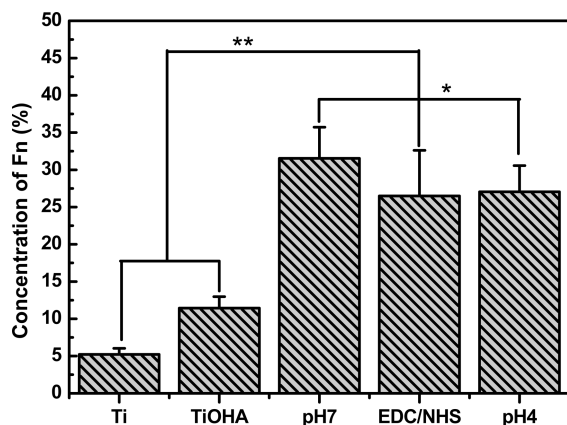


Figure 7. Quantitative characterization of fibronectin: determination of immobilized fibronectin on samples of pH 7, pH 4, and EDC/NHS by immunochemistry; pristine Ti and TiOHA were used as reference (** $p < 0.05$ compared with Ti and TiOHA; * $p > 0.05$ among different Hep/Fn immobilized samples; mean \pm SD, $N = 4$).

concentration of fibronectin was obtained on the surface of pH 7, pH 4, and EDC/NHS. However, no significant difference ($p > 0.05$) in fibronectin adsorption was observed between the samples of pH 7, pH 4, and EDC/NHS, indicating equivalent immobilization of fibronectin on these samples.

FITC-labeled antihuman fibronectin antibody was used to stain fibronectin immobilized on the samples. Fluorescence-microscopic images of the stained Hep/Fn films on pH 7, pH 4, and EDC/NHS are depicted in Figure 8. It can be seen that there

are fibronectin clusters with green color, in contrast with the TiOHA surface, which shows no staining using the same procedure. The results indicate that fibronectin was successfully immobilized on the samples. Nevertheless, no obvious difference was observed on the samples of pH 7, pH 4, and EDC/NHS, which was consistent with the results for fibronectin quantitation.

Hemolysis Rate. Hemolysis rate is an important parameter for the characterization of blood compatibility. The lower the hemolysis rate, the better the blood compatibility. Figure 9 shows the hemolysis rates of the Ti and Hep/Fn-immobilized surfaces. It can be seen that the hemolysis rates of the Hep/Fn-immobilized samples are significantly lower than that of Ti ($p < 0.05$). The hemolysis rate of Ti was $\sim 1.5\%$, whereas it was $<0.5\%$ for the Hep/Fn-immobilized samples, which is well below the accepted threshold value of 5%, implying good blood compatibility of Hep/Fn-immobilized surfaces. Other parameters can give some further information on blood compatibility.

APTT. The APTT test was performed to evaluate the anticoagulation activities of the samples. APTT corresponds to the intrinsic pathway of the blood-clotting system. APTT values for the samples of pH 7, pH 4, and EDC/NHS are shown in Figure 10. Ti and plasma were used as control and reference samples, respectively. It was found that the APTT values of all samples immobilized with Hep/Fn mixture were significantly prolonged compared with Ti and plasma ($p < 0.05$). The APTT values of all samples increased in the order: Ti $<$ plasma $<$ pH 7 = EDC/NHS $<$ pH 4. In addition, pH 4 had a significantly longer ($p < 0.05$) APTT value (~ 120 s) compared with the samples of pH 7 and EDC/NHS (~ 80 s), indicating better anticoagulation properties. No obvious difference was observed between the samples of pH 7 and EDC/NHS.

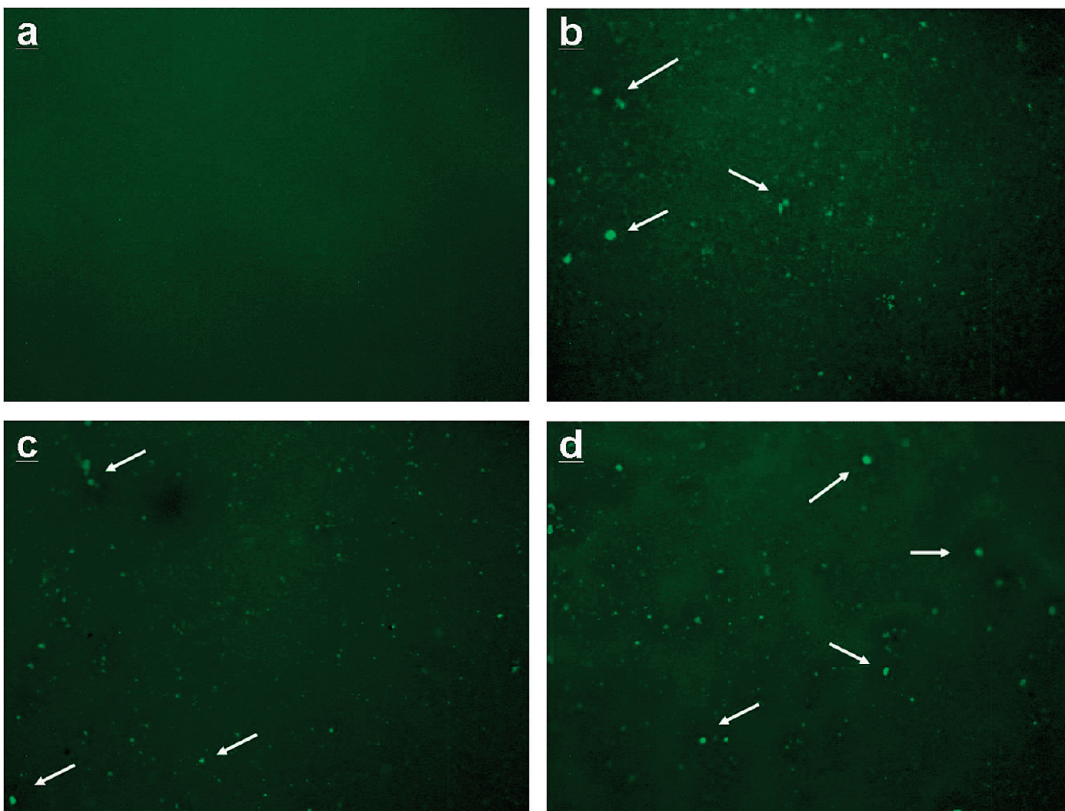


Figure 8. Qualitative characterization of fibronectin: fluorescence microscopic images of immunostained fibronectin sections of immobilized Hep/Fn on Ti surface: (a) TiOHA, (b) pH 7, (c) EDC/NHS, and (d) pH 4. Original magnification: 200 \times .

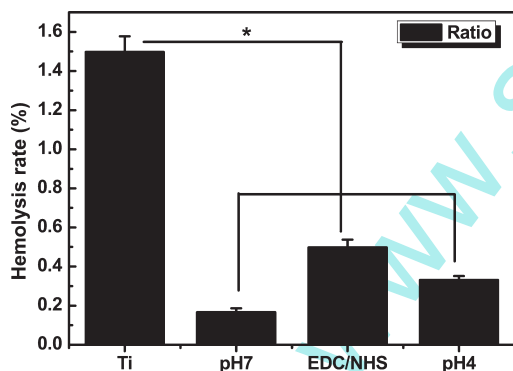


Figure 9. Hemolysis rate of the pristine Ti and Hep/Fn-immobilized samples (* $p < 0.05$ compared with Ti; mean \pm SD, $N = 4$).

Amount and Morphology of Adherent Platelets. The in vitro platelet adhesion test is used to investigate the blood compatibility of biomaterials. To study adhesion of platelets on different samples, we collected at least nine sight fields with the size of $5 \times 5 \mu\text{m}$ under a light microscope and counted adherent platelets for statistical analysis. The quantity of platelets on all samples after contact with PRP for 1 h is presented in Figure 11A. The data show that Ti facilitated a much higher level of platelet adhesion compared with samples of pH 7, pH 4, and EDC/NHS ($p < 0.05$). The quantity of adhered platelets on all the samples decreased in the order: Ti > pH 7 > EDC/NHS > pH 4. All Hep/Fn-immobilized samples showed two to three times fewer platelets compared with Ti. The sample of pH 4 displayed the smallest amount of adhered platelets, which was about three

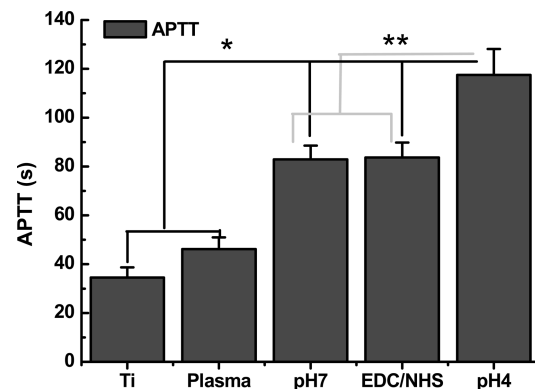


Figure 10. APTT values of Hep/Fn-immobilized surfaces: pH 7, pH 4, and EDC/NHS. The pristine Ti and plasma were used as reference (* $p < 0.05$ compared with Ti and plasma; ** $p < 0.05$ compared with pH 7 and EDC/NHS samples; mean \pm SD, $N = 4$).

times less than the Ti. This was in agreement with the anti-coagulation properties from the APTT results.

SEM images were used to evaluate the adhesion and morphology of platelets on various sample surfaces after incubation in PRP for 1 h. The representative typical images of platelets adhesion behavior on these surfaces are depicted in Figure 11B. Platelets adhered markedly on Ti with marked shape change (spreading) and pseudopod formation. However, platelet adhesion on Hep/Fn-immobilized surfaces was significantly reduced, and platelets maintained their round shapes with no formation of pseudopods (pH 7, EDC/NHS, and pH 4). No obvious shape

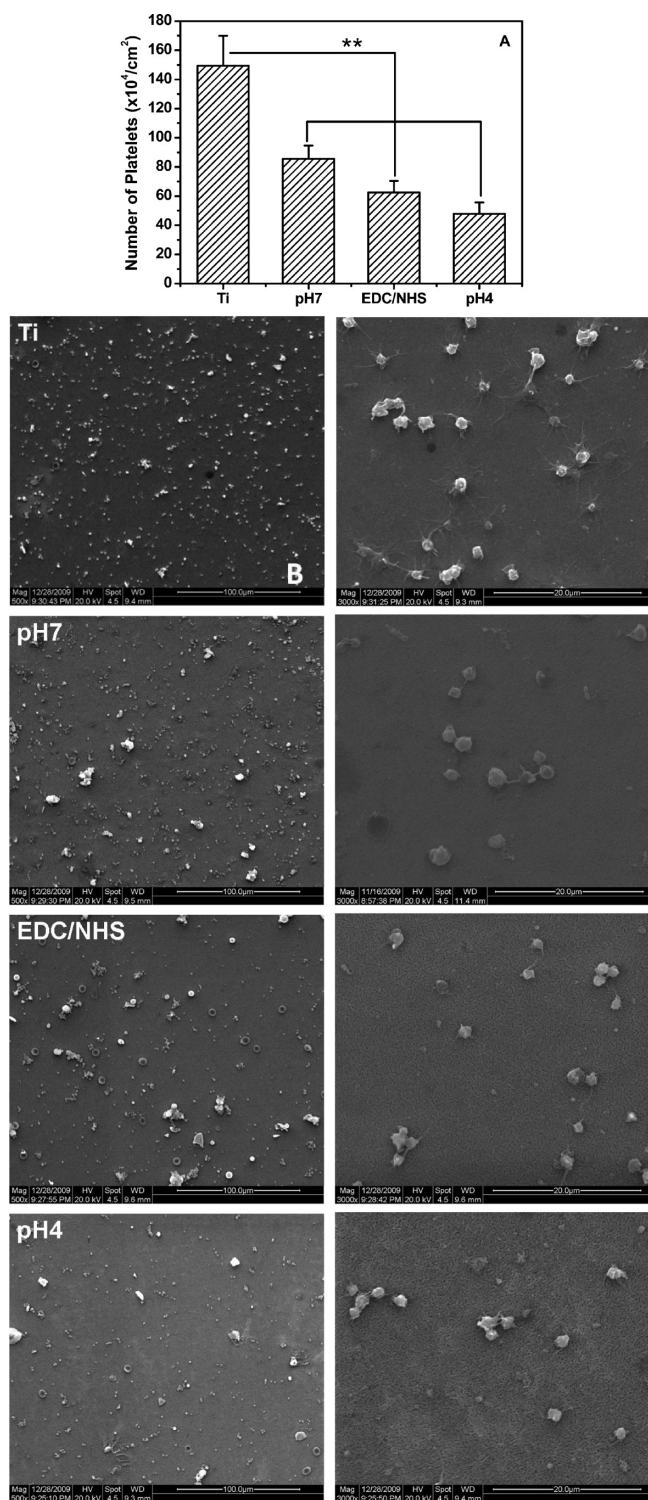


Figure 11. (A) Amount and (B) representative typical SEM photographs of platelets on pristine Ti, pH 7, EDC/NHS, and pH 4. The amount was obtained by counting adherent platelets under a light microscope (** $p < 0.05$ compared with Ti; mean \pm SD, $N = 9$).

difference of platelets on Hep/Fn-immobilized surfaces was observed, indicating that Hep/Fn-immobilized surfaces could not cause platelet activation.

Conformational Change of Fibrinogen γ Chain Exposure.

The conformational change in fibrinogen, that is, exposure of γ

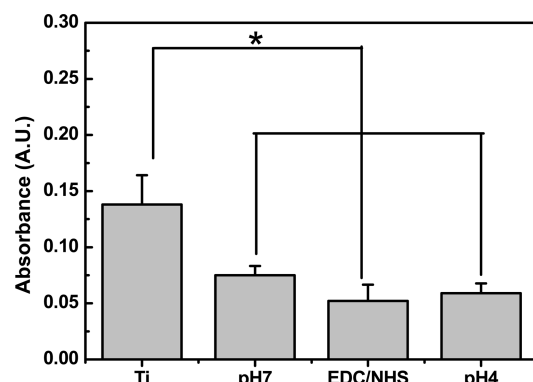


Figure 12. Conformational change of fibrinogen on different samples: pH 7, EDC/NHS, and pH 4. Ti was used as control (* $p < 0.05$ compared with Ti; mean \pm SD, $N = 4$).

chain (HHLGGAKQAGDV at γ 400–411),³⁸ plays a critical role in platelet activation and aggregation. Resting platelets interact with immobilized but not soluble fibrinogen. Fibrinogen is folded in plasma and no γ chain is exposed but is unfolded or conformationally changed when adsorbed on implants and the γ chain exposed. The exposure of γ chain promotes fibrinogen binding to the GPIIb/IIIa integrin receptor on the platelet membrane and causes further adhesion and aggregation of platelets.³⁹ Therefore, fibrinogen conformational changes measured by the immunoochemistry method could reveal the tendency to thrombosis. The conformational changes determined for all samples are shown in Figure 12. Samples of pH 7, EDC/NHS, and pH 4 show significantly smaller absorbance compared with Ti ($p < 0.05$). The results indicate that fibrinogens adsorbed on Ti surfaces underwent larger conformational changes than those on Hep/Fn-immobilized samples, suggesting a good blood compatibility of Hep/Fn-immobilized samples.

Proliferation and Morphology of EC. To detect the attachment and proliferation of endothelial cells on Hep/Fn-immobilized samples, ECs from human umbilical vein were seeded on the surface of different samples. After incubation for 1, 3, and 5 days, the quantity of EC was detected by the Alamar Blue test. Figure 13A shows the amount and proliferation of EC on the surface of Ti and on the surface immobilized with the Hep/Fn mixture. It can be seen that after culturing for 24 h, there is a higher EC count on the Hep/Fn-immobilized surfaces than on pristine Ti. The sample of pH 4 displayed larger amounts of EC than all other samples ($P < 0.05$). After culturing for 3 and 5 days, ECs on pH 4 and EDC/NHS surfaces proliferated faster than those on pristine Ti and pH 7 surfaces, whereas EC on pH 7 surface proliferated slower than those on pristine Ti surface. In addition, no obvious difference was observed between the samples of pH 4 and EDC/NHS on EC proliferation ($P > 0.05$), except for the 1 day culture. The results demonstrated that Hep/Fn-immobilized samples, pH 4 and EDC/NHS, could promote endothelial cell attachment and proliferation. This, however, depended on the different mixing conditions of heparin and fibronectin.

The proliferation and cytoskeletal arrangement of EC could be detected by immunofluorescence staining for actin expression. Figure 13B depicts the cytoskeleton of EC on different samples after incubation for 1, 3, and 5 days, respectively. The EC seeded on all samples exhibits elliptical, spherical, or polygonal morphology; aggregation only appears on the surface of EDC/NHS.

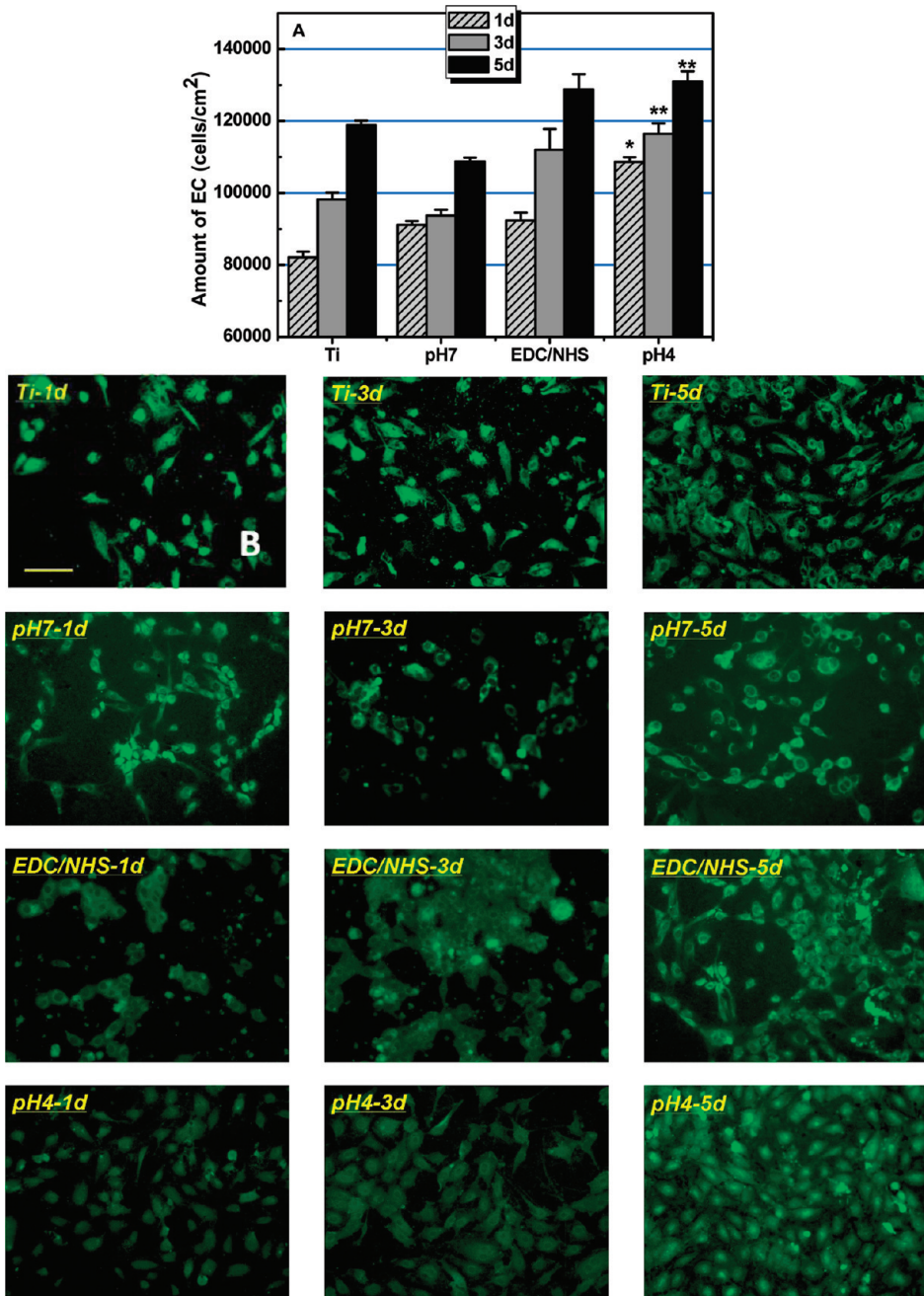


Figure 13. Amount and morphology of EC proliferation on pristine Ti and Hep/Fn-immobilized samples after incubation for 1, 3, and 5 days, respectively. (A) Alamar Blue test, * $P < 0.05$ compared with Ti, pH 7, and EDC/NHS; ** $P > 0.05$ compared to EDC/NHS; mean \pm SD, $N = 4$. (B) Actin staining of EC skeleton organization, error bar = 25 μ m.

The sample of pH 4 showed more EC attachment than the other samples on the first day. EC cultured on the surfaces of EDC/NHS and pH 4 displayed greater proliferation than those cultured on the surfaces of Ti and pH 7 by the third day. An increase in the amount of EC for all samples on the fifth day was observed. Compared with the 40% surface coverage on the third day, >70% of the surface of Ti was covered by EC by the fifth day. However, almost all of the surface of pH 4 was covered by EC with elliptic and cobblestone morphology by the fifth day, indicating an obvious cytoskeleton organization and proliferation on the surface of pH 4. EC on the samples of pH 7 and EDC/NHS also exhibited proliferation with rounded or congregated morphology,

which appeared different from their normal shape. These results show that the spreading and proliferation of ECs on the sample of pH 4 was enhanced. The sample of pH 4 thus performed better for endothelialization than others.

RGD Exposure of Fibronectin. To explore the mechanism of EC attachment and proliferation on Ti and the surface immobilized with Hep/Fn, we determined the exposure of RGD peptides on fibronectin using immunochemistry. The exposure of RGD peptides on fibronectin plays an important role in EC adhesion. RGD peptides can bind to the $\alpha 5\beta 1$ integrin receptor on the EC membrane and promote the attachment and spreading of EC. The exposure of RGD peptides on all samples is shown in Figure 14.

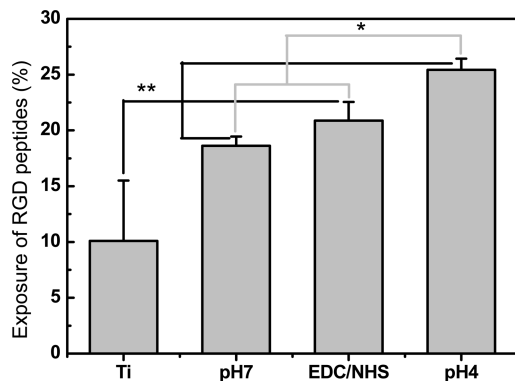


Figure 14. Exposure of RGD peptides on different samples determined by immunochemistry method. Ti was used as control (* $p < 0.05$ compared with pH 7 and EDC/NHS samples; ** $p < 0.05$ compared with Ti; mean \pm SD, $N = 4$).

It can be clearly seen that RGD peptide exposure on the Hep/Fn-immobilized surface is significantly higher than those on pristine Ti surface ($p < 0.05$). Additionally, the sample of pH 4 displays a significantly higher RGD exposure than the sample of pH 7 and EDC/NHS ($p < 0.05$), suggesting better endothelialization of pH 4 sample than pH 7 and EDC/NHS. The result is consistent with the Alamar Blue and cytoskeleton staining results.

■ DISCUSSION

The results presented in this study consistently demonstrated that covalent coimmobilization of Hep/Fn mixture can simultaneously improve blood compatibility and endothelialization of biomaterials, which would be of potentially great significance for long-term implantation of biomedical devices in the human body.

It is known that biocompatibility is the most important aspect of biomaterials implanted in the human body. Therefore, it is necessary to improve the biocompatibility of biomaterials using different methods, including physical and chemical modification and biomolecule immobilization. In this study, we used two biomolecules, heparin and fibronectin, which have the properties of anticoagulation and promotion of endothelial cell attachment, respectively, to construct a Hep/Fn coimmobilized surface for obtaining a good biocompatibility surface. The activated Ti surfaces (TiOH) and the Hep/Fn-immobilized surfaces (TiOHAHF) exhibited high hydrophilicity, whereas the APTE grafted surfaces (TiOHA) showed hydrophobicity; this could be ascribed to the hydrophilic groups on the surfaces of TiOH and TiOHAHF, such as hydroxyl groups, carboxyl groups, and so on, and the hydrophobic groups on the surfaces of TiOHA, such as methylene groups. The treatment of Ti in different stages gave rise to the different surface morphologies, from the smooth Ti surface to rough TiOH and TiOHA surfaces. Etching by NaOH created a rough Ti surface, and the grafting of the short chain alkyl of APTE further increased surface roughness. APTE can form a monolayer or a multilayer (polymerization) on the surface depending on the concentrations used.⁴⁰ The monolayer APTE could expose more amino groups than the multilayer, which could assist in the binding of carboxyl groups on biomolecules. APTE with higher concentrations in ethanol (>5%) may more readily form polymerized layers.⁴⁰ In our study, APTE at a concentration of 2% in ethanol was used; moreover, after grafting of APTE, the samples were sonicated in ethanol for 5 min to rinse the physisorbed APTE to achieve monolayer APTE adsorption.⁴⁰

However, the roughness of the TiOHA surfaces became less after the immobilization of Hep/Fn mixture, and these results may be caused by the filling of heparin and fibronectin molecules or by the cross-linking caused by the binding of Hep/Fn mixture to APTE. All NaOH activated, APTE grafted and biomolecule-immobilized surfaces appeared to be uniform on larger scans of $10 \times 10 \mu\text{m}$ but nonhomogeneous at the submicrometer range. No morphology differences were observed among the samples of pH 7, pH 4, and EDC/NHS.

We speculate from the above that heparin and fibronectin were coimmobilized on the surface. The quantitative (TBO, immunochemistry) and qualitative (FTIR, Alcian Blue, and immunostaining) characterization of heparin and fibronectin confirmed this possibility. Moreover, we found that after using electrostatic attraction (pH 4), heparin and fibronectin showed lower immobilization than that by EDC cross-linking (EDC/NHS) and pH 7 recognition. One reason may be that fibronectin had the heparin binding site at the fraction of FNIII_{12–14}.⁴¹ The interaction between heparin and fibronectin is mainly referable to hydrogen bonding and hydrophobic effects at physiological pH, and this would deplete carboxyl groups for heparin and fibronectin immobilization on the TiOHA surface. Another possible reason is the wettability difference because a hydrophilic surface may have a high affinity for heparin and fibronectin adsorption. Additionally, the different conditions that were used to combine heparin and fibronectin may have played an important role, with a further effect on the immobilization amount. Although the amount of heparin and fibronectin on the sample of pH 4 was not as great as that on the samples of pH 7 and EDC/NHS, it appeared enough for biological function, anticoagulation, and the promotion of endothelialization in the present study, in comparison with the studies by Toworfe et al.⁴²

The effect of heparin immobilization on Ti surface blood compatibility depends on both the extent of contact activation induced by the coimmobilized mixture and the anticoagulant properties of the biomodified bulk material. Ti per se could cause the contact activation of blood system and shorten the intrinsic clotting time.⁴³ However, the contact activation was markedly inhibited by the coimmobilized Hep/Fn mixture, indicated especially by the APTT and platelet adhesion tests. Platelet adhesion and aggregation is linked to fibrinogen; this protein is made up of three globular units connected by two rods. Each fibrinogen molecule has a dodecapeptide at the carboxyl terminus of the γ chain (HHLGGAKQAGDV at $\gamma_{400–411}$).³⁸ The dodecapeptide binds to the platelet integrin GPIIb/IIIa and was shown to be the most important site for mediating platelet adhesion and aggregation.³⁹ The samples immobilized with Hep/Fn mixture appeared to cause less conformational change of fibrinogen than the control Ti, which could be linked to platelet adhesion outcomes. Also, more recent results have demonstrated that the conformational alteration of fibrinogen is also higher after adsorption on hydrophobic surfaces than on hydrophilic surfaces.⁴⁴ The hydrophobic Ti surface showed the highest number of adherent platelets, and these adherent platelets were in a highly activated state. In contrast, the more hydrophilic Hep/Fn-immobilized surfaces showed a small number of adherent and activated platelets. Nevertheless, for all samples immobilized with Hep/Fn, the results of the conformational change of fibrinogen were not consistent with the results of the contact angles. This may be because processes other than wettability, such as the surface physicochemical change, may also influence this process.

Additionally, it was interesting to note that the sample of pH 4 displayed the longest APTT value and the lowest quantity of platelets, indicating better blood compatibility than the other samples, that is, pH 7 and EDC/NHS, although the quantity of heparin immobilized on this sample was not the highest. It appears that the anticoagulation properties of heparin are not altered or influenced when heparin combines with fibronectin by electrostatic attraction, although the quantity immobilized is affected. Immobilized heparin on a material surface was reported to inactivate factor XIIa in the presence of ATIII,⁴⁵ whereas fibronectin is an adhesion molecule for the binding site of the platelet facilitating platelet adhesion.⁴⁶ From the results of blood compatibility, we tentatively put forward the hypothesis that the anticoagulant property of heparin is not influenced by fibronectin, whereas the coagulation induction properties of fibronectin are inhibited by the heparin. A possible mechanism for this is that the binding of heparin to fibronectin interferes with its conformational change and that some binding sites for platelets are inhibited. However, this needs further study.

As would be expected, a large amount of the immobilized fibronectin would increase the attachment of endothelial cells because of the cell-binding domains in the protein structure. However, the quantity of endothelial cells did not correlate well with the fibronectin quantity on the samples of pH 7, EDC/NHS, and pH 4. It is hypothesized that the conformational change of fibronectin and exposure of the cell-binding domains might be more influenced when heparin and fibronectin are combined at the physiological pH 7, therefore affecting the attachment of endothelial cells, whereas the exposure of cell-binding domains was less affected under conditions of pH 4 and EDC/NHS. A parallel experiment to detect the exposure of cell-binding domains, that is, RGD peptides, using immunochemistry method confirmed this hypothesis. Fibronectin immobilized on the surface of pH 4 showed significantly higher exposure of RGD peptides compared with that on the surface of pH 7 and EDC/NHS ($p < 0.05$). This suggests that the cell-binding activity of fibronectin would not be reduced when heparin and fibronectin are combined by electrostatic attraction, whereas cell-binding activity of fibronectin on Hep/Fn films is reduced when heparin and fibronectin combine under physiologic conditions and when there is cross-linked combination, indirectly seen in the EC 1 day culture.

Cell spreading and shape, which are related to surface wetting,⁴⁷ topography,^{48–50} and physicochemistry properties,^{51–54} are important modulators of cellular function. It was observed in the present study that endothelial cells on the surface of Ti and on pH 4 showed flattening and their plasma membrane spread on the substratum, whereas on the surface of pH 7 and EDC/NHS, endothelial cells still showed a rounded morphology, characteristic of initial attachment after culturing on the biomaterial surface, and aggregation. The shape of a cell is closely related to cells function. Normally, an endothelial cell in a vein wall has a spindle or oval shape, presenting a better biological function, and proliferation only occurs for cells that are spread out. The rounded endothelial cells or aggregates would inhibit their proliferation and biological function and may even show apoptosis.^{50,55} Also, the topography of all surfaces here are equivalent and could be excluded as a variable, so we speculate that the physicochemical properties, linked to the immobilized biomolecules, dominated cells behavior. Notably, cell spreading was greatly enhanced on the surface of pH 4 from 1, 3, to 5 days. The combination of heparin and fibronectin by electrostatic attraction under pH 4

appears to play a crucial role in this cell effect. However, it is notable that after EDC/NHS cross-linking, heparin and fibronectin cause the endothelial cells clustering, and cell structure was also different from that on other samples. Interestingly, our results are not consistent with the study by Wissink et al.,⁵⁶ who found a large degree of endothelial cell proliferation using EDC/NHS cross-linked collagen on polyethylene terephthalate (PET) substrate. It is not clear why cross-linking of heparin and fibronectin causes the congregation of endothelial cells. Possibly, the cross-linking effect of EDC/NHS on various biomolecules is different, and the different substrates and the cross-linking methods may also lead to the differences of cell proliferation, which needs further study.

Short-term good blood compatibility (1 h) and endothelialization (5 days) have been simultaneously obtained by coimmobilizing Hep/Fn mixture on Ti surface under static conditions; although the mechanism underlying this is still not clear, simultaneous immobilization of different types of biomolecules is recommended. Further studies are required to evaluate the stability and bioactivity of coimmobilized Hep/Fn mixtures under flow conditions and to evaluate interaction mechanism between substrate-immobilized biomolecules and platelets/endothelial cells.

CONCLUSIONS

Heparin and fibronectin could be readily coimmobilized on silanized Ti surfaces and their bioactivities retained. Co-immobilization of heparin and fibronectin gave favorable blood compatibility and endothelialization, simultaneously. The combination of heparin and fibronectin by electrostatic attraction gave much better bioactivity and biocompatibility than under physiological conditions and using the EDC/NHS cross-linking system. This method can be extended to other biomolecules immobilized on different biomaterials or tissue engineering grafts. To conclude, the present surface biomodification technology may offer a potential improvement for implanted cardiovascular devices.

AUTHOR INFORMATION

Corresponding Author

*Tel: +86 028 8763 4148 802. Fax: +86 028 8760 0625. E-mail: yangpingswjt@163.com.

ACKNOWLEDGMENT

We gratefully acknowledge the financial support of Fundamental Research Funds for the Central Universities (2010XS32), Key Basic Research Program (2011CB606204), National Physiological Science Foundation of China (30870629), and NSFC-RGC (30831160509) and the kind language assistance from Professor Pankaj Vadgama (England), Professor Ian Brown (U.S.), Miss Jie Liu, Dr. Zhilu Yang, Lisa Schoeller (Germany), and Matt Mlamore (U.S.).

REFERENCES

- (1) Williams, D. F. On the mechanisms of biocompatibility. *Biomaterials* **2008**, *29*, 2941–2953.
- (2) Balasubramanian, V.; Hall, C. L.; Shivashankar, S.; Slack, S. M.; Turitto, V. T. Vascular cell attachment and procoagulant activity on metal alloys. *J. Biomater. Sci., Polym. Ed.* **1998**, *9*, 1349–1359.
- (3) Pfisterer, M.; Brunner-La Rocca, H. P.; Buser, P. T.; Rickenbacher, P.; Hunziker, P.; Mueller, C.; Jeger, R.; Bader, F.; Osswald, S.; Kaiser, C.

- Late clinical events after clopidogrel discontinuation may limit the benefit of drug-eluting stents: an observational study of drug-eluting versus bare-metal stents. *J. Am. Coll. Cardiol.* **2006**, *48*, 2584–2591.
- (4) Plant, S. D.; Grant, D. M.; Leach, L. Behaviour of human endothelial cells on surface modified NiTi alloy. *Biomaterials* **2005**, *26*, S359–S367.
- (5) Hauert, R. A review of modified DLC coatings for biological applications. *Diamond Relat. Mater.* **2003**, *12*, 583–9.
- (6) Huang, N.; Yang, P.; Leng, Y. X.; Chen, J. Y.; Sun, H.; Wang, J.; Zhao, A. S. Hemocompatibility of titanium oxide films. *Biomaterials* **2003**, *24*, 2177–2187.
- (7) Baldwin, S. P.; Saltzman, W. M. Polymers for tissue engineering. *Trends Polym. Sci.* **1996**, *4*, 177–182.
- (8) Weber, N.; Wendel, H. P.; Ziener, G. Hemocompatibility of heparin-coated surfaces and the role of selective plasma protein adsorption. *Biomaterials* **2002**, *23*, 429–439.
- (9) Gong, F. R.; Cheng, X. Y.; Wang, S. F.; Zhao, Y. C.; Gao, Y.; Cai, H. B. Heparin-immobilized polymers as non-inflammatory and non-thrombogenic coating materials for arsenic trioxide eluting stents. *Acta Biomater.* **2010**, *6*, 534–546.
- (10) Zhu, A. P.; Zhang, M.; Wu, J.; Shen, J. Covalent immobilization of chitosan/heparin mixture with a photosensitive hetero-bifunctional crosslinking reagent on PLA surface. *Biomaterials* **2002**, *23*, 4657–4665.
- (11) Chiu, L. L. Y.; Radisic, M. Scaffolds with covalently immobilized VEGF and Angiopoietin-1 for vascularization of engineered tissues. *Biomaterials* **2010**, *31*, 226–241.
- (12) Yin, Y. B.; Wise, S. G.; Nosworthy, N. J.; Waterhouse, A.; Bax, D. V.; Youssef, H.; Byrom, M. J.; Bilek, M. M.; McKenzie, D. R.; Weiss, A. S. Covalent immobilisation of tropoelastin on a plasma deposited interface for enhancement of endothelialisation on metal surfaces. *Biomaterials* **2009**, *30*, 1675–1681.
- (13) Muller, R.; Abke, J.; Schnell, E.; Macionczyk, F.; Gbureck, U.; Mehrl, R.; Ruszczak, Z.; Kujat, R.; Englert, C.; Nerlich, M.; Angele, P. Surface engineering of stainless steel materials by covalent collagen immobilization to improve implant biocompatibility. *Biomaterials* **2005**, *26*, 6962–6972.
- (14) Hersel, U.; Dahmen, C.; Kessler, H. RGD modified polymers: biomaterials for stimulated cell adhesion and beyond. *Biomaterials* **2003**, *24*, 4385–4415.
- (15) Nojiri, C.; Noishiki, Y.; Koyanagi, H. Aorta-coronary bypass grafting with heparinised vascular grafts in dogs. *J. Thorac. Cardiovasc. Surg.* **1987**, *93*, 867–877.
- (16) Stemberger, A.; Ascherl, R.; Blumel, G. Kollagen ein biomaterial in der medizin. *Hämostaseologie* **1990**, *10*, 164–76.
- (17) Parise, P.; Agnelli, G. Thrombus resistance to lysis and reocclusion after thrombolysis: the role of platelets. *Blood Coagulation Fibrinolysis* **1991**, *2*, 749–758.
- (18) Wang, X. Y.; Zhang, X. H.; Castellot, J.; Herman, I.; Iafrati, M.; Kaplan, D. L. Controlled release from multilayer silk biomaterial coatings to modulate vascular cell responses. *Biomaterials* **2008**, *29*, 894–903.
- (19) Meng, S.; Liu, Z. J.; Shen, L.; Guo, Z.; Chou, L. L.; Zhong, W.; Du, Q. G.; Ge, J. B. The effect of a layer-by-layer chitosan–heparin coating on the endothelialization and coagulation properties of a coronary stent system. *Biomaterials* **2009**, *30*, 2276–2287.
- (20) Rigberg, D.; Tulloch, A.; Chun, Y.; Mohanchandra, K. P.; Carman, G.; Lawrence, P. Thin-film nitinol (NiTi): a feasibility study for a novel aortic stent graft material. *J. Vasc. Surg.* **2009**, *50*, 375–380.
- (21) Middleton, C. A.; Pendegrass, C. J.; Gordon, D.; Jacob, J.; Blunn, G. W. Fibronectin silanized titanium alloy: a bioinductive and durable coating to enhance fibroblast attachment in vitro. *J. Biomed. Mater. Res., Part A* **2007**, *83*, 1032–1038.
- (22) Wang, X. H.; Li, D. P.; Wang, W. J.; Feng, Q. L.; Cui, F. Z.; Xu, Y. X.; Song, X. H. Covalent immobilization of chitosan and heparin on PLGA surface. *Int. J. Biol. Macromol.* **2003**, *33*, 95–100.
- (23) Guarneri, D.; De Capu, A.; Ventre, M.; Borzacchiello, A.; Pedone, C.; Marasco, D.; Ruvo, M.; Netti, P. A. Covalently immobilized RGD gradient on PEG hydrogel scaffold influences cell migration parameters. *Acta Biomater.* **2010**, *6*, 2532–2539.
- (24) Uygun, B. E.; Stojsih, S. E.; Matthew, H. W. T. Effects of immobilized glycosaminoglycans on the proliferation and differentiation of mesenchymal stem cells. *Tissue Eng., Part A* **2009**, *15*, 3499–3512.
- (25) Adil, D. Heparin-immobilized poly(2-hydroxyethylmethacrylate)-based microspheres. *J. Appl. Sci.* **1999**, *74*, 655–662.
- (26) Ruoslahti, E. Structure and biology of proteoglycans. *Annu. Rev. Cell Biol.* **1988**, *4*, 229–255.
- (27) Damus, P. S.; Hicks, M.; Rosenberg, R. B. Anticoagulant action of heparin. *Nature* **1997**, *246*, 355–357.
- (28) Bos, G. W.; Scharenborg, N. M.; Poot, A. A.; Engbers, G. H. M.; Beugeling, T.; Aken, W. G.; van Feijen, J. Proliferation of endothelial cells on immobilized albumin-heparin conjugate loaded with basic fibroblast growth factor. *J. Biomed. Mater. Res.* **1999**, *44*, 330–340.
- (29) Potts, J. R.; Campbell, I. D. Structure and function of fibronectin modules. *Matrix Biol.* **1996**, *15*, 313–320.
- (30) Pankov, R.; Yamada, K. M. Fibronectin at a glance. *J. Cell. Sci.* **2002**, *115*, 3861–3863.
- (31) Lee, M. H.; Ducheyne, P.; Lynch, L.; Boettiger, D.; Composto, R. J. Effect of biomaterial surface properties on fibronectin-alpha(5)beta(1) integrin interaction and cellular attachment. *Biomaterials* **2006**, *27*, 1907–1916.
- (32) Cho, J. Y.; Mosher, D. F. Enhancement of thrombogenesis by plasma fibronectin cross-linked to fibrin and assembled in platelet thrombi. *Blood* **2006**, *107*, 3555–3563.
- (33) Luyn, M. J. A.; Van, P.; Wachem, P. B.; Van, L.; Olde Damink, L. H. H.; Dijkstra, P. J.; Feijen, J. Relations between in vitro cytotoxicity and crosslinked dermal sheep collagens. *J. Biomed. Mater. Res.* **1992**, *26*, 1091–1110.
- (34) Wachem, P. B.; van, P.; Luyn, M. J. A.; van, L.; Olde Damink, L. H. H.; Dijkstra, P. J.; Feijen, J.; Nieuwenhuis, P. Tissue regenerating capacity of carbodiimide-crosslinked dermal sheep collagen during repair of the abdominal wall. *Biomaterials* **1994**, *17*, 230–239.
- (35) Wissink, M. J. B.; Beernink, R.; Pieper, J. S.; Poot, A. A.; Engbers, G. H. M.; Beugeling, T.; Aken, W. G.; van, P.; Feijen, J. Immobilization of heparin to EDC/NHS-crosslinked collagen. Characterization and in vitro evaluation. *Biomaterials* **2001**, *22*, 151–163.
- (36) Richert, L.; Lavalle, P.; Payan, E.; Shu, X. Z.; Prestwich, G. D.; Stoltz, J. F.; Schaaf, P.; Voegel, J. C.; Picart, C. Layer by layer buildup of polysaccharide films: physical chemistry and cellular adhesion aspects. *Langmuir* **2004**, *20*, 448–458.
- (37) Smith, R. K.; Mallia, A. K.; Hermanson, G. T. Colorimetric method for the assay of heparin content in immobilized heparin preparations. *Anal. Biochem.* **1980**, *109*, 466–473.
- (38) Kloczewiak, M.; Timmons, S.; Lukas, T. J.; Hawiger, J. Platelet receptor recognition site on human-fibrinogen—synthesis and structure function relationship of peptides corresponding to the carboxyterminal segment of the gamma-chain. *Biochemistry* **1984**, *23*, 1767–1774.
- (39) Tsai, W. B.; Grunkemeier, J. M.; Horbett, T. A. Variations in the ability of adsorbed fibrinogen to mediate platelet adhesion to polystyrene-based materials: a multivariate statistical analysis of antibody binding to the platelet binding sites of fibrinogen. *J. Biomed. Mater. Res., Part A* **2003**, *67*, 1255–1268.
- (40) Suri, C. R.; Mishra, G. C. Activating piezoelectric crystal surface by silanization for microgravimetric immunobiosensor application. *Biosens. Bioelectron.* **1996**, *11*, 1199–1205.
- (41) Peterson, J. A.; Sheibani, N.; David, G.; Garcia-Pardo, A.; Peters, D. M. Heparin II domain of fibronectin uses $\alpha 4\beta 1$ integrin to control focal adhesion and stress fiber formation, independent of syndecan-4. *J. Biol. Chem.* **2005**, *280*, 6915–6922.
- (42) Toworfe, G. K.; Composto, R. J.; Adams, C. S.; Shapiro, I. M.; Ducheyne, P. Fibronectin adsorption on surface-activated poly(dimethylsiloxane) and its effect on cellular function. *J. Biomed. Mater. Res., Part A* **2004**, *71*, 449–461.
- (43) Hong, J.; Andersson, J.; Ekdahl, K. N.; Elgue, G.; Axén, N.; Larsson, R.; Nilsson, B. Titanium is a highly thrombogenic biomaterial: possible implications for osteogenesis. *Thromb. Haemostasis* **1999**, *82*, 58–64.

- (44) Roach, P.; Farrar, D.; Perry, C. C. Interpretation of protein adsorption:surface-induced conformational changes. *J. Am. Chem. Soc.* **2005**, *127*, 8168–8173.
- (45) Sanchez, J.; Elgue, G.; Riesenfeld, J.; Ollson, P. Control of contact activation on end point immobilized heparin: the role of antithrombin and the specific antithrombin-binding sequence. *J. Biomed. Mater. Res.* **1995**, *29*, 655–661.
- (46) Tsai, W. B.; Grunkemeier, J. M.; McFarland, C. D.; Horbett, T. A. Platelet adhesion to polystyrene-based surfaces preadsorbed with plasmas selectively depleted in fibrinogen, fibronectin, vitronectin, or von Willebrand's factor. *J. Biomed. Mater. Res.* **2002**, *60*, 348–359.
- (47) Frisch, T.; Thoumine, O. Predicting the kinetics of cell spreading. *J. Biomech.* **2002**, *35*, 1137–1141.
- (48) Chen, C. S.; Mrksich, M.; Huang, S.; Whitesides, G. M.; Ingber, D. E. Geometric control of cell life and death. *Science* **1997**, *276*, 1425–1428.
- (49) Paul, N. E.; Skazik, C.; Harwardt, M.; Bartneck, M.; Denecke, B.; Klee, D.; Salber, J.; Klarwasser, G. Z. Topographical control of human macrophages by a regularly microstructured polyvinylidene fluoride surface. *Biomaterials* **2008**, *29*, 4056–4064.
- (50) Morelli, S.; Salerno, S.; Piscioneri, A.; Papenburg, B. J.; Vito, A. D.; Giusi, G.; Canonaco, M.; Stamatialis, D.; Drioli, E.; Bartolo, L. D. Influence of micro-patterned PLLA membranes on outgrowth and orientation of hippocampal neurites. *Biomaterials* **2010**, *31*, 7000–7011.
- (51) Toworfe, G. K.; Bhattacharyya, S.; Composto, R. J.; Adams, C. S.; Shapiro, I. M.; Ducheyne, P. Effect of functional end groups of silane self-assembled monolayer surfaces on apatite formation, fibronectin adsorption and osteoblast cell function. *J. Tissue Eng. Regener. Med.* **2009**, *3*, 26–36.
- (52) Keselowsky, B. G.; Collard, D. M.; Garcia, A. J. Surface chemistry modulates fibronectin conformation and directs integrin binding and specificity to control cell adhesion. *J. Biomed. Mater. Res., Part A* **2003**, *66*, 247–259.
- (53) Wittmer, C. R.; Phelps, J. A.; Saltzman, W. M.; Van Tassel, P. R. Fibronectin terminated multilayer films: protein adsorption and cell attachment studies. *Biomaterials* **2007**, *28*, 851–860.
- (54) Shi, D. Y.; Ma, D.; Dong, F. Q.; Zong, C.; Liu, L. Y.; Shen, D.; Yuan, W. J.; Tong, X. M.; Chen, H. W.; Wang, J. F. Proliferation and multi-differentiation potentials of human mesenchymal stem cells on thermo-responsive PDMS surfaces grafted with PNIPAAm. *Biosci. Rep.* **2010**, *30*, 149–158.
- (55) Grigoriou, V.; Shapiro, I. M.; Cavalcanti-Adam, E. A.; Composto, R. J.; Ducheyne, P.; Adams, C. S. Apoptosis and survival of osteoblast-like cells are regulated by surface attachment. *J. Biol. Chem.* **2005**, *280*, 1733–1739.
- (56) Wissink, M. J. B. Endothelialization of Collagen Matrices-Endothelial cell seeding on crosslinked collagen: Effects of crosslinking on endothelial cell proliferation and functional parameters. Thesis, University of Twente, Enschede, The Netherlands, 1999.